Effect of the Shape of Geometric Discontinuity on Nature of Rayleigh Wave Back Reflection

M. Šofer [1,a], P. Ferfecki [2], J. Neugebauer [3]

[1] *VŠB - Technical University of Ostrava, Department of Applied Mechanics, Czech Republic*
[2] *VŠB - Technical University of Ostrava, IT4Innovations, Czech Republic*
[3] *PTS Josef Solnař s.r.o., Czech Republic*
[a] *michal.sofer@vsb.cz*

Abstract: The aim of our study is to show the influence of the shape of a particular type of the geometric discontinuity on the nature of Rayleigh wave back reflection. Experiments were carried out with aim of ultrasonic equipment from Olympus company, namely with Epoch 600 digital ultrasonic flaw detector and 1 MHz transducers with wedge in order to generate Rayleigh wave in used steel samples. COMSOL Multiphysics software has been used to simulate the propagation of Rayleigh wave on tested geometry as well as to estimate the losses of energy due to back reflection on tested geometric discontinuities.

Keywords: Rayleigh wave; ultrasound; geometric discontinuity; finite element method.

1 Introduction

Non-destructive testing (NDT) is nowadays widely used for various technical applications. Ultrasonic testing, as one of NDT methods, is based on the propagation of ultrasonic waves in tested object or material. From a mathematical point of view, there exist two types of waves: the bulk waves and the surface waves [1]. Bulk waves travel through the interior of the medium while surface waves propagate only at the interface between two different media. Although bulk and surface waves are fundamentally different, they are governed by the same set of partial differential wave equations [2]. The difference is, that for bulk waves, there are no boundary conditions, which need to be satisfied. Rayleigh waves, as one of the types of surface waves, are widely used in various NDT applications. Rayleigh waves are the result of interfering longitudinal and shear waves, the particle motion (Fig. 1) of the wave in the case of homogenous medium and moving from left to right is elliptical in a counter-clockwise direction along the free surface [3]. Generally, Rayleigh waves are used for detection of the surface and near-surface cracks in industrial practice. The penetration depth of surface wave is approximately equal to its wavelength and is strongly dependent on the frequency of the wave [2].

The main aim of proposed paper is to provide an experimental and a numerical study, dealing with the influence of the shape of particular type of geometric discontinuity on the nature of Rayleigh wave´s back reflection.

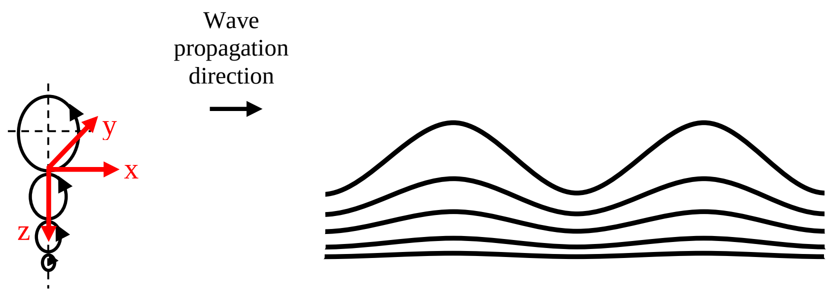

Fig. 1: Particle motion during wave propagation.

2 Mathematical Description of Rayleigh Wave Propagation Along Free Surface

The origin of mathematical relations for displacements in *x* and *z*-axis of Rayleigh surface wave propagation along the free surface is realised by an assumption of isotropic, homogeneous, linear elastic semi-space. The motion is defined as two-dimensional so that all quantities are independent on *y* coordinate. The displacement vector $\bar{u}$ can be with the use of Helmholtz decomposition defined as follows

$$\bar{u} = \nabla \cdot \phi + \nabla \times \bar{\psi} \,. \tag{1}$$

Where ϕ is a potential function, and $\bar{\psi}$ is a vector function, and this functions are defined in the following form

$$\phi = \phi(x,z) \,,\ \bar{\psi} = (0, -\psi(x,z), 0) \,. \tag{2}$$

The equation of motion expressed in terms of displacements

$$\mu \cdot \nabla^2 \cdot \bar{u} + (\lambda + \mu) \cdot \nabla \cdot (\bar{\nabla} \cdot \bar{u}) = \rho \cdot \ddot{\bar{u}} \tag{3}$$

can be separated into two wave equations, one for dilatational waves and one for shear waves

$$\nabla^2 \phi - \frac{1}{c_L^2} \cdot \ddot{\phi} = 0 \,,\ \nabla^2 \psi - \frac{1}{c_T^2} \cdot \ddot{\psi} = 0 \,. \tag{4}$$

μ and λ are Lame's constants, ρ is the mass density per unit volume, c_L is the wave speed of dilatational waves, c_T is the wave speed of shear waves, $(\cdot\cdot)$ denotes the second derivative with respect to time, and $(\bar{\ })$ denotes complex conjugation.

Let for both functions consider harmonic wave motion in form of $\phi = \Phi(z) \cdot e^{i(\omega t - kx)}$, $\psi = \Psi(z) \cdot e^{i(\omega t - kx)}$ and following boundary conditions of the components of the stress tensor on the free surface must be met $\sigma_z = \tau_{xz} = \tau_{zy} = 0$, then it is possible to derive the horizontal *u* and vertical *v* displacements

$$u = A \cdot k \cdot \left(e^{-q \cdot z} - \frac{2 \cdot q \cdot s}{s^2 + k^2} \cdot e^{-q \cdot z} \right) \cdot \sin(\omega \cdot t - k \cdot x), \tag{5}$$

$$w = A \cdot q \cdot \left(e^{-q \cdot z} - \frac{2 \cdot k^2}{s^2 + k^2} \cdot e^{-q \cdot z} \right) \cdot \cos(\omega \cdot t - k \cdot x), \tag{6}$$

$$s = \sqrt{k^2 \left(1 - \left(\frac{c_S^2}{c_T^2} \right) \right)} \,,\ q = \sqrt{k^2 \left(1 - \frac{1 - 2\nu}{2 - 2\nu} \left(\frac{c_S^2}{c_T^2} \right) \right)} \,. \tag{7}$$

A is a constant, which influences the amplitude of the wave, *k* is the wavenumber, c_S is the wave speed of surface waves, ω is the frequency, *t* is time, and ν is Poisson´s ratio.

3 Experimental Procedure

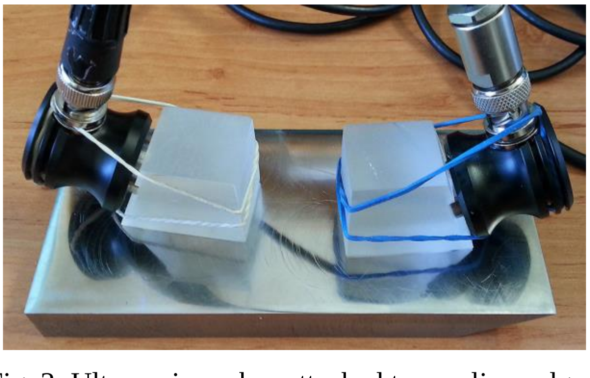

Fig. 2: Ultrasonic probes attached to acrylic wedges.

Experiments were carried out with the use of ultrasonic equipment from Olympus company, namely with Epoch 600 digital ultrasonic flaw detector and 1 MHz transducers with self-manufactured wedges in order to generate Rayleigh wave in used steel samples (Fig. 2).

Altogether, four measurements with different geometry shape in terms of the inclination angle φ, namely 60, 90, 120, and 150 degrees (Fig. 3) have been realised. All specimens were produced from the steel grade CSN 11 523 with the thickness of 15 mm, width of 65 mm, and length of 130 mm.

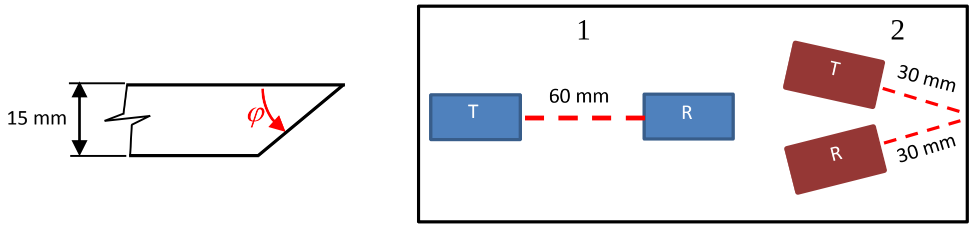

Fig. 3: Scheme of the measurement procedures (T-transducer, R-receiver).

The measurement is composed of two steps: (1) the measurement of an echo on the free surface, which is used as a reference measurement, and (2) the measurement of an echo, generated by back reflection (Fig. 3). The loss of echo related to the back reflection and compared to free surface is defined as follows:

$$L_{ech} = \left(1 - \frac{E_{re}}{E_{fs}}\right) \cdot 100\% \,. \tag{8}$$

L_{ech} is the loss of echo, E_{re}, E_{fs} are the echo heights (re – reflected, fs – free surface) in percentage for the stated gain, and the peaks of the oscillation in the case of numerical simulations, respectively. Needless to say, that the echo from edge back reflection had to be recalculated on the same gain value, which was used in case of measuring echo for free surface according to:

$$\Delta A = 20 \cdot \log\left(\frac{H_1}{H_2}\right), \tag{9}$$

where ΔA represents the gain in dB, and H_1, H_2 are the echo heights in percentage.

4 Results of the Numerical Simulations

Rayleigh surface wave propagation of the shape of a particular type was performed by means of a finite element code COMSOL Multiphysics. The loss of echo was obtained by solving of 2D wave propagation problem for the specified size of the inclination angle on the geometric discontinuity. The investigated specimens are made of steel with the elastic modulus of $2.0 \cdot 10^{11}$ Pa, Poisson's ratio of 0.33, and the density of 7850 kg·m^{-3}.

The boundary condition of the prescribed displacement in the horizontal and vertical direction is defined according to Eqs. (5-6). In Fig. 4, the boundary condition is specified by the green coloured line.

In the computational model, the specimen was discretized by quadratic quadrilateral elements. The total number of degrees of freedom of the discretized specimen is approximately equal to 700 000, and its value depends on the size of inclination angle.

A generalized-alpha method for integrating of the equation of motion was applied to obtain the transient propagation of the Rayleigh surface wave.

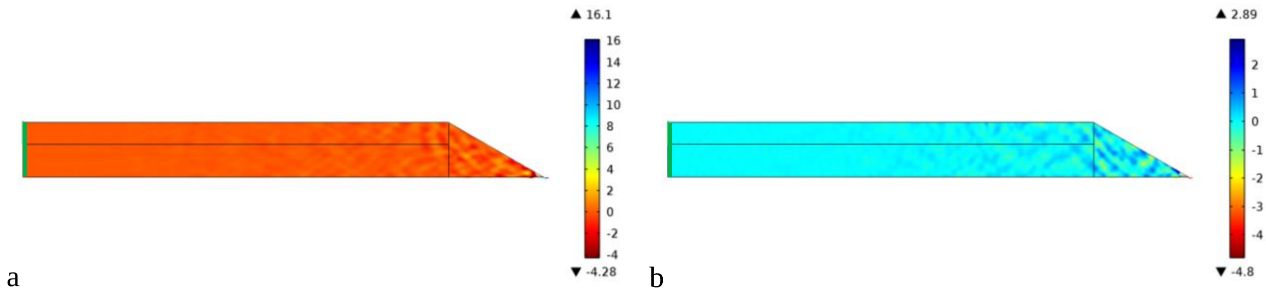

Fig. 4: Displacement in the direction-x (a) and displacement in the direction-y (b).

The distribution of the horizontal (a) and the vertical (b) displacement for the specimen with inclination angle equal to 150 degrees at time of 51.5 μs is drawn in Fig. 4. The loss of echo is determined at this time point.

5 Comparison of the Numerical and Experimental Results

Time history of the numerically computed vertical displacement component of the point on the specimen's surface in the case of the inclination angle of 60, 90 degrees and 120, 150 degrees is drawn in Figs. 5a, 5b. The peaks of the oscillation corresponding to the primary and reflected wave in the time course are indicated. The exact position of the peaks of oscillation has been determined according to the wave velocity.

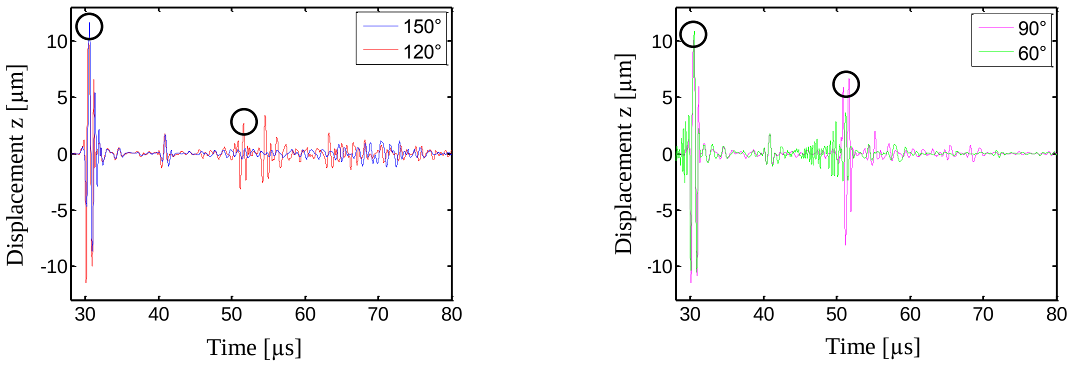

Fig. 5: History of the displacement.

The measured and the computed loss of echo of the specimens with different shape of the inclination angle are shown in Table 1. The inclination angle larger than 90 degrees will cause a significant change in the loss of echo.

Table 1: The measured and computed loss of echo.

φ [°]	60	90	120	150
$L_{ech,mea}$ [%]	35	47	81	98
$L_{ech,sim}$ [%]	34	40	73	97

6 Conclusion

Good agreement has been obtained between results of the numerical simulations and the experimental measurements in terms of analysis of Rayleigh wave back reflection on geometric discontinuities. The future work will be focused on improving the experimental and numerical procedures in order to obtain closer results between used approaches. Authors will also focus on problematics of Rayleigh wave back reflection on different configuration of surface cracks.

Acknowledgement

This work was supported by Specific Research (SP2016/145) and by The Ministry of Education, Youth and Sports from the National Programme of Sustainability II (LQ1602). The support is acknowledged.

References

[1] M. H. Sadd, Wave Motion and Vibration in Continuous Media, Kingston, University of Rhode Island, 2009.

[2] J. L. Rose, Ultrasonic Waves in Solid Media, Cambridge, Cambridge University Press, 2002.

[3] L. Rayleigh, On waves propagated along the plane surface of an elastic solid, Proceedings London Mathematical Society 17 (1885), 4–11.